Centralized Multi-user Multi-rate Haptic Cooperation Using Wave Transformation

Naser Yasrebi
Department of Mechanical Engineering
University of Victoria
Victoria, BC, V8W 3P6 Canada
nyasrebi@me.uvic.ca

Daniela Constantinescu
Department of Mechanical Engineering
University of Victoria
Victoria, BC, V8W 3P6 Canada
danielac@me.uvic.ca

***Abstract*—This paper proposes a multi-rate control strategy for multi-user haptic cooperation. In the proposed architecture, the virtual environment simulation runs on a central server to which all users are connected as clients. Users send position commands to and receive forces from the centralized virtual object that they cooperatively manipulate via wave-based controllers. After deriving the passivity condition for the multi-rate wave transformation, the paper investigates the stability of the cooperation between two users within a multi-rate discrete-time state space framework. The analysis predicts that clients can cooperatively manipulate much stiffer centralized virtual objects when connected to the server using wave transformations than when connected using virtual coupling. Experiments performed in a 1 degree of freedom (DOF) virtual environment confirm the analytical results.**

***Index Terms*—Multi-rate multi-user haptic cooperation, centralized control.**

I. Introduction

Force feedback can enhance task performance in haptic applications that require the cooperation of multiple users [1]. Regardless of potential advantages and important applications [2], [3], [4], [5], haptic cooperation over network/Internet remains a research challenge because several factors severely degrade its stability and transparency. These factors include time delay in the communication channels [6], packet loss [7], low communication bandwidth [8], [9].

Much experimental research has addressed networked haptic cooperation. The study in [6] has shown that time delay decreases stability and performance in collaborative haptic systems. Two peer-to-peer and one client-server architectures have been compared through interactions between users connected via Internet in [9]. All those three architectures are based on virtual coupling [10] coordination, and have been used to evaluate the effect of network conditions on their performance. An NIST Net network emulator has simulated varying time delay and thus, Internet-based communications in [11]. Virtual coupling-based peer-to-peer and client-server architectures have been contrasted in terms of position coherency, and a distributed scheme with position coherency comparable to centralized schemes has been proposed in [12]. For peer-to-peer communications, virtual coupling and wave variable controllers have been demonstrated to maintain higher position coherency and lower force errors that time domain passivity-based controllers [13].

The stability of centralized and distributed cooperative haptic systems under constant communication delay has been analyzed in [8] using the state space multi-rate modeling introduced in [14]. The analysis has proven centralized cooperation doomed to instability unless limited contact stiffness is rendered to client users when they are connected to the centralized virtual environment via virtual coupling.

The use of wave variable control for stabilizing sampled data systems has also been a recent research focus. Wave transformations between virtual environment variables and the haptic device variables have been studied through modeling delays only in the return path in [15]. Our analysis shows that analytical results change significantly with the location of the delay. Wave transformations between virtual environment variables and motor variables have been employed in [16] after incorporating the motor dynamics into the system model. Wave-based haptic interaction with a slow molecular docking simulation has been proposed in [17], but required additional virtual damping to remain stable. In [18], wave domain communications between a slow virtual environment and a haptic device have been proven passive inclusive of the downsampler and the upsampler in the absence of aliasing.

This paper proposes centralized haptic cooperation with multi-rate wave transformations for coping with fixed time delays and slow network update rates. In the proposed architecture, the virtual environment simulation runs on a central server to which all users are connected as clients. Users send position commands to and receive forces from the centralized virtual object that they cooperatively manipulate via wave-based controllers. The paper starts by deriving the passivity condition for the multi-rate wave transformations in Section II. The continuous time model of cooperation between two users is derived in Section III, followed by the stability analysis of its discrete time counterpart in Section IV. The stability region of the multi-rate system is derived in Section VI. Experimental results validating the analysis are included in Section VIII. The paper ends with conclusions and directions for future work.

II. Multirate wave transformation

A passive system can not generate energy, i.e., a system with effort (force) $f(t)$, flow (velocity) $v(t)$, and initial energy $E(0)$ obeys [19]:

$$\int_0^t f(t)v(t)dt + E(0) \geq 0. \tag{1}$$

In other words, passive systems dissipate at least as much energy as they generate. Wave transformations have been shown to preserve the passivity of communication channels with time delay in both the continuous [20] and the discrete [21] domains. This section derives the passitivy condition for muli-rate wave transformations (Figure 1).

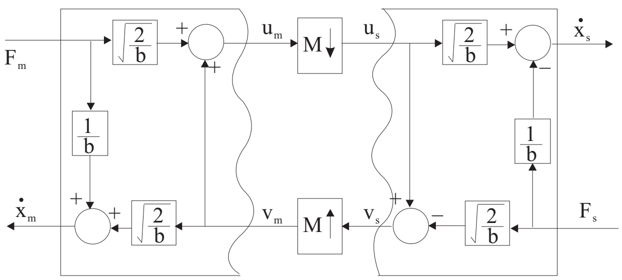

Fig. 1. A sampled-data system with downsampling and upsampling in the communication channels.

The discrete domain energy balance in the communication channels can be written as:

$$\Delta E = \sum_{n=0}^{n=N_f} [\frac{1}{2}(u_m^T(n)u_m(n)T - u_s^T(n)u_s(n)MT) + \frac{1}{2}(v_s^T(n)v_s(n)MT - v_m^T(n)v_m(n)T)]. \tag{2}$$

where N_f is the number of samples. The second term in Equation (2) is zero. Indeed the upsampling does not inject energy to the system:

$$\frac{1}{2}\sum_{n=0}^{n=N_f} [v_s^2(n)MT - v_m^2(n)T] = 0 \tag{3}$$

Since ZOH expander was used as the upsampler, the following relation holds:

$$v_m(n+m) = v_s(n), \quad for \ 0 \leq m < M \tag{4}$$

Using Equation (4) gives:

$$\Sigma v_s^2(n)MT = \Sigma v_m^2(n)T \tag{5}$$

which proves the second term in Equation (2) is equal to zero.

For the first term in Equation (2) applying Parseval's theorem gives:

$$\Sigma u_s^2(n)MT = \frac{TM}{2\pi}\int_{-\pi}^{\pi} |U_s(e^{\omega j})|^2 d\omega \tag{6}$$

by assuming no aliasing, i.e., $U_s(j\omega) = \frac{1}{M}U_m(e^{\frac{j\omega}{M}})$ for $|\omega| < \frac{\pi}{M}$:

$$\frac{TM}{2\pi}\int_{-\pi}^{\pi} |U_s(e^{\omega j})|^2 d\omega = \frac{T}{2\pi M}\int_{-\pi}^{\pi} |U_m(e^{\frac{\omega j}{M}})|^2 d\omega \tag{7}$$

By defining $\frac{\omega}{M} = \omega_1$ Equation (7) becomes:

$$\frac{T}{2\pi}\int_{\frac{-\pi}{M}}^{\frac{\pi}{M}} |U_m(e^{\omega_1 j})|^2 d\omega_1 = \Sigma u_m^2(n)T \tag{8}$$

Which implies that the first term in Equation (2) is equal to zero, by this assumption that the aliasing does not occur. When aliasing happens the first term in Equation (2) is not equal to zero and it can be positive or negative. Hence to gaurantee the passivity of the communication channel, it is necessary to prevent the aliasing.

By using a LP filter with cutoff frequency less than $\frac{\pi}{M}$ before the downsampler, it is possible to prevent the aliasing and gaurantee the passivity of the system.

III. Stability of a haptic centralized cooperation system with multirate wave transformation

Figure 2 shows a centralized cooperative haptic system with 2 users in which the users can manipulate a cube cooperatively.

The dynamics of the networked haptic shown in Figure 2 are, for notations refer to the Appendix:

- for the client HDs (device motion and virtual contact forces balanced by the user force F_{hi}):

$$m_{\text{HD1}}\ddot{x}_1 + b_{\text{HD}}\dot{x}_1 = F_{\text{h1}} - F_1 \tag{9}$$

$$m_{\text{HD2}}\ddot{x}_2 + b_{\text{HD}}\dot{x}_2 = F_{\text{h2}} - F_2 \tag{10}$$

- for the VO :

$$m_{\text{O}}\ddot{x}_{\text{O}} + b_{\text{O}}\dot{x}_{\text{O}} = F_{\text{s1}} + F_{\text{s2}} \tag{11}$$

where F_1 and F_2 are shown in Figure 2.

Instead of transmitting the power variables F_{s1}, F_{s2}, $\dot{x}_1$, and $\dot{x}_2$, the following wave variables are transmitted between the server and the clients:

$$u_{\text{ci}} = \sqrt{2b}\dot{x}_{\text{i}} - v_{\text{ci}}, \quad i = 1,2 \tag{12}$$

$$v_{\text{si}} = u_{\text{si}} + \frac{-F_{\text{si}}}{\sqrt{2b}}, \quad i = 1,2 \tag{13}$$

where b is the wave impedance and the following relations hold between wave variables:

$$u_{\text{si}}(t) = u_{\text{ci}}(t - T_d)(M\downarrow), \quad i = 1,2 \tag{14}$$

$$v_{\text{ci}}(t) = v_{\text{si}}(t - T_d)(M\uparrow), \quad i = 1,2 \tag{15}$$

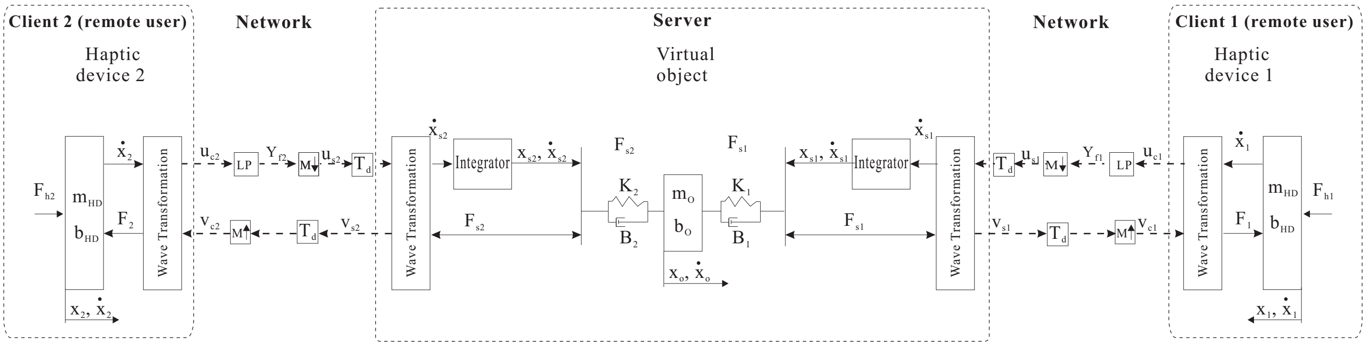

Fig. 2. Model of the centralized single-axis cooperative haptics.

The force applied on the users , F_1 and F_2, is computed using the following relation:

$$F_{\mathrm{i}} = b\dot{x}_{\mathrm{i}} - \sqrt{2b}v_{\mathrm{ci}}, \quad i = 1,2 \tag{16}$$

for finding $F_{\mathrm{si}},\ i = 1,2$, at first the corresponding velocity of device i, on the server side is computed by decoding the wave variables:

$$\dot{x}_{\mathrm{si}} = \frac{2}{\sqrt{b}}u_{\mathrm{si}} + \frac{-F_{\mathrm{si}}(t - T_{VE})}{b}, \quad i = 1,2 \tag{17}$$

next, by integrating $\dot{x}_{\mathrm{si}}$ in discrete domain, x_{si} is found. Finally F_{si} is equal to:

$$F_{\mathrm{si}} = K_{\mathrm{i}}(x_{\mathrm{si}} - x_{\mathrm{O}}) + B_{\mathrm{i}}(\dot{x}_{\mathrm{si}} - \dot{x}_{\mathrm{O}}), \quad i = 1,2 \tag{18}$$

As it is shown in Equation (16), F_{i} is comprised of two terms: $b\dot{x}_i$ and $-\sqrt{2b}v_{\mathrm{ci}}$. By using these terms in place of F_{i} the continuous state space model of the system becomes:

$$\dot{\mathbf{x}}_{6\times1} = \mathbf{A}_{6\times6}\dot{\mathbf{x}}_{6\times1} + \mathbf{B}_{6\times6}\mathbf{u}_{6\times1} \tag{19}$$

where :

$$\mathbf{u^T}_{6\times1} = \begin{pmatrix} F_{\mathrm{b1}} & F_{\mathrm{b2}} & v_{\mathrm{c1}} & v_{\mathrm{c2}} & F_{\mathrm{s1}} & F_{\mathrm{s2}} \end{pmatrix} \tag{20}$$

and $F_{\mathrm{bi}} = b\dot{x}_i$. The output of the system is:

$$\mathbf{y}_{6\times1} = \mathbf{C}_{6\times6}\mathbf{x}_{6\times1} \tag{21}$$

where $\mathbf{C}$ is 6×6 unity matrix.

As mentioned earlier, the haptic cooperation system in Figure 2 is not a continuous-time system. Rather, it is:

- a sampled-data system because of the discrete nature of the virtual environment simulation.
- a system with multiple rates because of the inherent limitations of the communication port (specifically, data from remote clients is read at frequencies of 128Hz, and the local control loop runs at 1024Hz).

Therefore, its stability will be investigated using the multirate sampled systems state space modeling approach proposed in [14].

IV. Discrete time state-space dynamics of haptic cooperation

To derive the multi-rate state space model the states, outputs, and inputs vectors are expanded in the following manner [14], Figure 3:

- The multi-rate state vector for the discrete-time system with dynamics given in Equation (19) is, Figure 3(c):

$$\mathbf{x}_{\mathrm{D}_{48\times1}}[k] \quad = \quad \begin{pmatrix} \mathbf{x}_{6\times1}\left(\left(k-1\right)T_0 + \tau_0\right) \\ \mathbf{x}_{6\times1}\left(\left(k-1\right)T_0 + 2\tau_0\right) \\ \vdots \\ \mathbf{x}_{6\times1}\left(\left(k-1\right)T_0 + 7\tau_0\right) \\ \mathbf{x}_{6\times1}\left(kT_0\right) \end{pmatrix} \tag{22}$$

- The outputs (positions & velocities) measured at the control sampling rate T_c for haptic cooperation are, Figure 3(b):

$$\mathbf{y}_{\mathrm{D}_{c_{48\times1}}}[k] \quad = \quad \begin{pmatrix} \mathbf{y}_{6\times1}\left(kT_0\right) \\ \mathbf{y}_{6\times1}\left(kT_0 + T_c\right) \\ \vdots \\ \mathbf{y}_{6\times1}\left(kT_0 + 7T_c\right) \end{pmatrix} \tag{23}$$

The outputs (positions & velocities) measured at the network sampling rate T_n for haptic cooperation are:

$$\mathbf{y}_{\mathrm{D}_{n_{6\times1}}}[k] \quad = \quad \begin{pmatrix} \mathbf{y}_{6\times1}\left(kT_0\right) \end{pmatrix} \tag{24}$$

The augmented output vector is:

$$\mathbf{y}_{\mathrm{D}_{54\times1}}[k] = \begin{pmatrix} \mathbf{y}_{\mathrm{D}_{c_{48\times1}}}[k] \\ \mathbf{y}_{\mathrm{D}_{n_{6\times1}}}[k] \end{pmatrix} \tag{25}$$

- The augmented input vector includes, Figure 3(a): The augmented input vector that depends on positions and velocities measured locally at the control sampling rate

T_c:

$$\mathbf{u}_{\mathrm{D}_{c_{16\times1}}}[k] = \begin{pmatrix} F_{\mathrm{b1}}\left(kT_0\right) \\ F_{\mathrm{b2}}\left(kT_0\right) \\ \vdots \\ F_{\mathrm{b1}}\left(kT_0+7T_c\right) \\ F_{\mathrm{b2}}\left(kT_0+7T_c\right) \end{pmatrix} = \mathbf{F}_{16\times1}[k] \tag{26}$$

and the augmented input vector at the network sampling rate T_n:

$$\mathbf{u}_{\mathrm{D}_{n_{4\times1}}}[k] = \begin{pmatrix} v_{\mathrm{c1}}\left(kT_0\right) \\ v_{\mathrm{c2}}\left(kT_0\right) \\ F_{\mathrm{s1}}\left(kT_0\right) \\ F_{\mathrm{s2}}\left(kT_0\right) \end{pmatrix} \tag{27}$$

Hence:

$$\mathbf{u}_{\mathrm{D}_{20\times1}}[k] = \begin{pmatrix} \mathbf{F}_{16\times1}[k] \\ v_{\mathrm{c1}}[k] \\ v_{\mathrm{c2}}[k] \\ F_{\mathrm{s1}}[k] \\ F_{\mathrm{s2}}[k] \end{pmatrix} \tag{28}$$

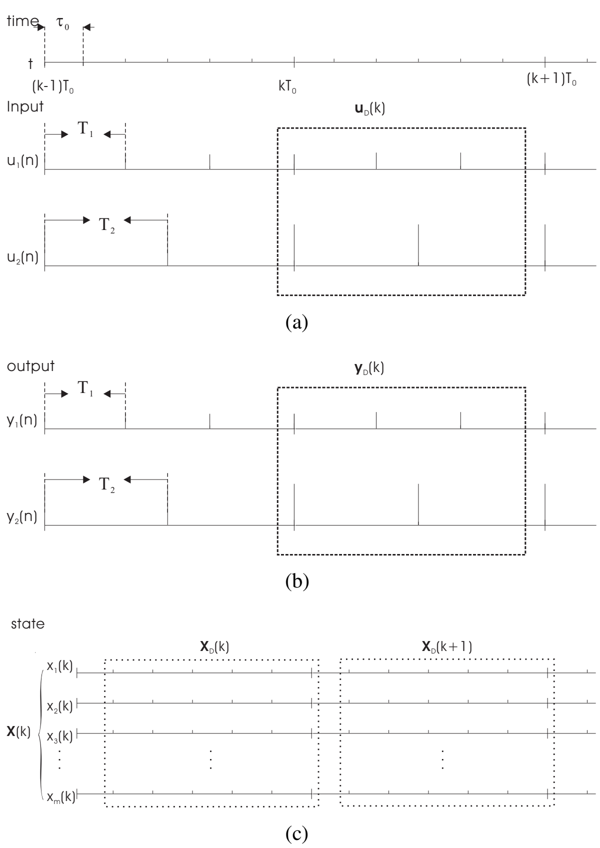

Fig. 3. Expanded vectors [14].

The discrete-time state-space dynamics of the multi-rate centralized haptic cooperation system are:

$$\mathbf{x}_{\mathrm{D}}[k+1] = \mathbf{A}_{\mathrm{D}}\mathbf{x}_{D}[k] + \mathbf{B}_{\mathrm{D}}\mathbf{u}_{\mathrm{D}}[k] \tag{29}$$

The output equation is:

$$\mathbf{y}_{\mathrm{D}}[k] = \mathbf{C}_{\mathrm{D}}\mathbf{x}_{\mathrm{D}}[k] + \mathbf{D}_{\mathrm{D}}\mathbf{u}_{\mathrm{D}}[k] \tag{30}$$

For more details about $\mathbf{A}_{\mathrm{D}}$, $\mathbf{B}_{\mathrm{D}}$, $\mathbf{C}_{\mathrm{D}}$, $\mathbf{D}_{\mathrm{D}}$ and how they are related to the continues model matrices refer to[14].

V. Including wave transformation in state-space model

Incorporating the wave transformation into the state-space model is done through the following steps :

- the wave variable v_{ci} is used as one of the system inputs, Equation (19).
- considering $\dot{x}_{\mathrm{s1}}$, x_{s1}, $\dot{x}_{\mathrm{s2}}$, and x_{s2} as the system states and augmenting u_{s1} and u_{s2} into the inputs of the system, by using :

$$\begin{aligned} \dot{x_{\mathrm{si}}}(k+1) &= \frac{K_{\mathrm{i}}(x_{\mathrm{si}}(k)-x_{\mathrm{O}}(k))}{b} \\ &+ \frac{B_{\mathrm{i}}(\dot{x}_{\mathrm{si}}(k)-\dot{x}_{\mathrm{O}}(k))}{b} + u_{si}(k) \end{aligned} \tag{31}$$

$$x_{\mathrm{si}}(k+1) = (T_n)\dot{x_{\mathrm{si}}}(k) + x_{\mathrm{si}}(k)$$

- adding $\mathbf{u}_{\mathrm{ci}}$, v_{si}, and F_{si} into the system outputs according to the Equation (12), Equation (13), and Equation (18) respectively:
- As shown in Section II, a low pass filter before the down-sampler is required to guarantee the passivity of the system with multi-rate wave transformations. The continuous time state space model of the fist order low pass filter is:

$$\begin{aligned} \dot{x}_{\mathrm{fi}} &= -50x_{\mathrm{fi}} + u_{\mathrm{fi}} \\ y_{\mathrm{fi}} &= 50x_{\mathrm{fi}} \end{aligned} \tag{32}$$

The multi-rate model of the filter is as follow, which is derived by using the same method used for constructing multi-rate model of the system:

$$\begin{aligned} \mathbf{x}_{\mathrm{fi}_{8\times1}}[k+1] &= \mathbf{A}_{\mathrm{fi}_{8\times8}}\mathbf{x}_{\mathrm{fi}_{8\times1}}[k] + \mathbf{B}_{\mathrm{fi}_{8\times8}}\mathbf{u}_{\mathrm{fi}_{8\times1}} \\ \mathbf{y}_{\mathrm{fi}_{9\times1}}[k] &= \mathbf{C}_{\mathrm{fi}_{9\times8}}\mathbf{x}_{\mathrm{fi}_{8\times1}}[k] + \mathbf{D}_{\mathrm{fi}_{9\times8}}\mathbf{u}_{\mathrm{fi}_{8\times1}} \end{aligned} \tag{33}$$

After integrating the multi-rate state space model of the filters with the multi-rate state-space model of the haptic system, the input-output relationship becomes:

- the fast part of u_{ci}, the fist 8 elements, are the filter input:

$$\mathbf{u}_{\mathrm{fi}_{8\times1}} = \mathbf{u}_{\mathrm{ci}}(1\rightarrow 8) \tag{34}$$

- the slowly updated part of the filter output, the last element of $\mathbf{y}_f$, is equal to u_{s2}:

$$u_{\mathrm{si}} = \mathbf{y}_{\mathrm{fi}}(9) \tag{35}$$

- v_{ci} is equal to v_{si}
- F_{si} is related to the outputs, according to Equation (18).

VI. Stability Analysis

To check the stability of the closed loop system, the closed loop state matrix for each pair of (K_1 , K_2) is found and the magnitude of its largest eigenvalue is checked according to the stability criterion:

$$\left\| Eig(\mathbf{A}_{\text{Dnew}} + \mathbf{B}_{\text{Dnew}}\mathbf{F}_{\text{D}}(\mathbf{I} - \mathbf{D}_{\text{Dnew}}\mathbf{F}_{\text{D}})^{-1}\mathbf{C}_{\text{Dnew}}) \right\| < 1 \tag{36}$$

where $\mathbf{A}_{\text{Dnew}}$, $\mathbf{B}_{\text{Dnew}}$, $\mathbf{C}_{\text{Dnew}}$, $\mathbf{D}_{\text{Dnew}}$ are the new state space model matrices after incorporating the wave variables and augmenting the filter dynamics, and $\mathbf{F}_{\text{D}}$ is the feedback matrix. The delays were incorporated in the state space model by augmenting the delayed inputs in the state vector [8]. All virtual damping couplers are equal to 10 Ns/m, wave impedance is equal to 20 Ns/m and no damping is considered for the devices.

The stability region for virtual coupler parameters, K_1 and K_2, are shown in Figure 4 for different time delays T_d. As shown in these figures increasing time delay slightly changes the stability region.

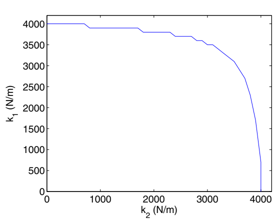

(a) $T_d = 0$

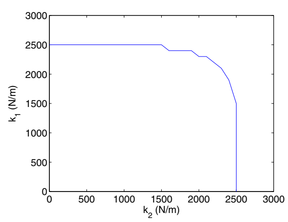

(b) $T_d = T_n$

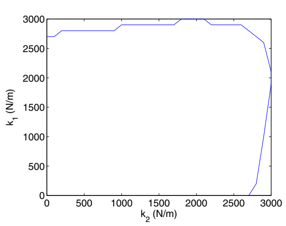

(c) $T_d = 2T_n$

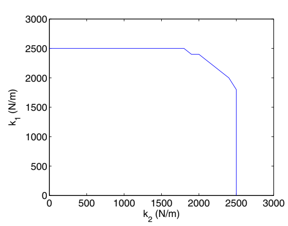

(d) $T_d = 3T_n$

Fig. 4. Stability region for a slowly updated centralized haptic system. The haptic control rate is $T_c = \frac{1}{1024}$ s, and the network update rate is $T_n = \frac{1}{128}$ s.

VII. Experimental results

This section presents experiments performed using a client Phantom Omni haptic device interacting with a server virtual wall. The results represent the case of a single user interacting with a fixed virtual cube via the control architecture depicted in Figure 2. The face of the cube touched by the user is located at $x = 0$. In the experiment, a constant force is applied as the user input at the handle of the haptic device. The position of the haptic interface x_m, the position command in the virtual environment x_s, and the force applied to the user F_m are shown in Figure 5 for two time delays, $T_d = 0.01$ s, 0.02 s. Figure 5 validates that stiff contacts can be rendered to the user in the presence of the two constant time delays. The impedance perceived by the user during contact, $\frac{F_m}{x_m}$, is approximately equal to 1000 N/m, which is the stiffness of the cube in the virtual environment. This result demonstrates the suitable performance of the proposed wave-based controller in terms of transparency.

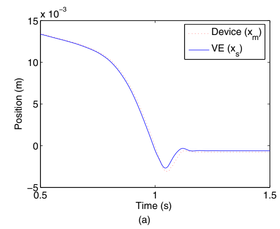

(a) The position of the haptic device (dotted) and x_s (solid), $T_d = 0.01$ s, $b = 20$ Ns/m.

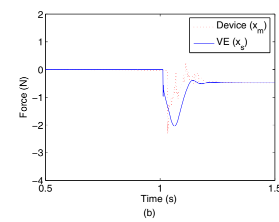

(b) Corresponding forces.

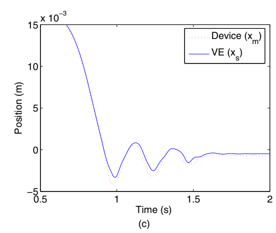

(c) the position of the haptic (dotted) and x_s (solid), $T_d = 0.02$ s, $b = 25$ Ns/m.

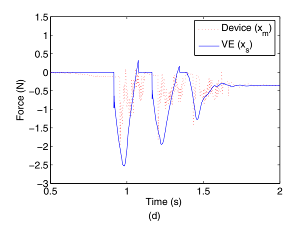

(d) Corresponding forces.

Fig. 5. Experimental result for $K_1 = 1000$ N/m.

VIII. Conclusions

This paper has proposed wave-based communications for centralized haptic cooperation. It has also shown: (1) that multi-rate wave transformations are passive only in the absence of aliasing; and (2) that wave-based control can render large contact stiffness in the presence of significant constant communication delays (Figure 4). A comparison of wave-based centralized haptic cooperation(Figure 4) to virtual coupling-based centralized cooperative haptics [8] (Figure 6) shows the much larger stability region of multi-rate wave-based control. The importance of this result becomes apparent when considering that centralized haptic cooperation may be required by a number of applications because of the size or the cost of the virtual environment software.

The proposed approach is restricted to haptic cooperation in the presence of constant network delay and constant update rate. Many methodologies have been proposed for coping with varying time delays in the literature [22], [23], [24], [25]. Upcoming work will investigate the use of robust control for maintaining centralized haptic cooperation systems stable in the presence of varying time delays and varying update rates.

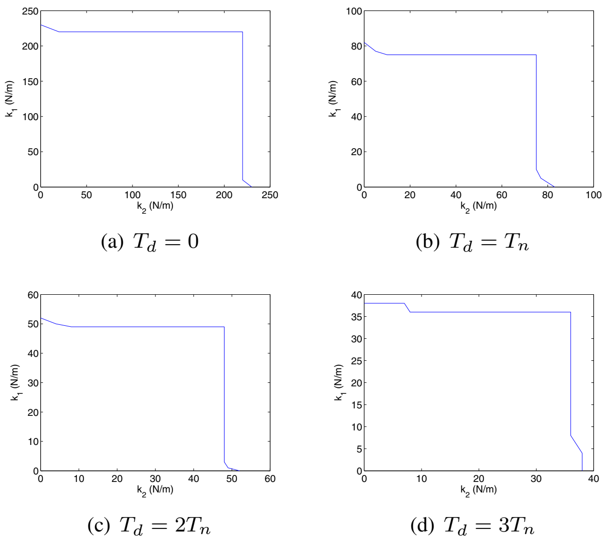

(a) $T_d = 0$ (b) $T_d = T_n$

(c) $T_d = 2T_n$ (d) $T_d = 3T_n$

Fig. 6. Stability region for centralized haptic cooperation with virtual coupling [8], $T_n = \frac{1}{128}$.

References

[1] X. Shen, J. Zhou, A. E. Saddik, and N. D. Georganas. Architecture and evaluation of tele-haptic environments. In *8th IEEE Int. Symp. Distr. Simu. Real Time Applic.*, pages 53–60, Budapest, Hungary, 2004.

[2] M. Osama and A. S. Horiguchi. Tele-handshake: A cooperative shared haptic virtual environment. In *EuroHaptics 2001*, pages 60–64, Birmingham, UK, 2001.

[3] C. Gunn, M. Hutchins, D. Stevenson, M. Adcock, and P. Youngblood. Using collaborative haptics in remote surgical training. In *IEEE Symp. Haptic Interf. Virt. Envir. Teleop. Syst.*, pages 481–482, Pisa, Italy, 2005.

[4] H.R. Choi, B.H. Choi, and S.M. Ryew. Haptic display in the virtual collaborative workspace shared by multiple users. In *6th IEEE Int. Workshop Robot Human Communic.*, pages 478–483, Sendai, Japan, 1997.

[5] J. P. Hespanha, M. Mclaughlin, G. S. Sukhatme, M. Akbarian, R. Garg, and W. Zhu. Haptic collaboration over the internet. In *Fifth Phantom Users Group Workshop*, pages 9–13, New York City, NY, USA, 2000.

[6] M. O. Alhalabi, S. Horiguchi, and S. Kunifuji. An experimental study on the effects of network delay in cooperative shared haptic virtual environment. *Comput. Graph.*, 27(2):205 – 213, 2003.

[7] S. Hirche and M. Buss. Packet loss effects in passive telepresence systems. In *IEEE Conf. Dec. Control*, pages 4010–4015, Atlantis, Paradise Island, Bahamas, 2004.

[8] M. Fotoohi, Sh. Sirouspour, and D. Capson. Stability and Performance Analysis of Centralized and Distributed Multi-rate Control Architectures for Multi-user Haptic Interaction. *Int. J. Robot. Res.*, 26(9):977–994, 2007.

[9] G. Sankaranarayanan and B. Hannaford. Experimental Internet Haptic Collaboration using Virtual Coupling Schemes. In *IEEE Symp. Haptic Interf. Virt. Envir. Teleop. Syst.*, pages 259–266, Reno, NE, USA, 2008.

[10] J.E. Colgate, M.C. Stanley, and J.M. Brown. Issues in the haptic display of tool use. In *IEEE/RSJ Int. Conf. Intell. Robots Syst.*, page 3140–3145, Pittsburgh, PA, USA, 1995.

[11] G. Sankaranarayanan and B. Hannaford. Comparison of performance of virtual coupling schemes for haptic collaboration using real and emulated internet connections. In *1st Int. Conf. Robot. Communic. Coordination*, pages 1–8, Athens, Greece, 2007.

[12] G. Sankaranarayanan and B. Hannaford. Virtual coupling schemes for position coherency in networked haptic environments. *IEEE/RAS-EMBS Int. Conf. Biomed. Robot. Biomechatronics*, pages 853–858, Pisa, Italy, 2006.

[13] G. Sankaranarayanan and B. Hannaford. Experimental comparison of internet haptic collaboration with time-delay compensation techniques. *IEEE Int. Conf. Robot. Autom.*, pages 206–211, Pasadena, CA, USA, 2008.

[14] M. Araki and K. Yamamoto. Multivariable multirate sampled-data systems: State-space description, transfer characteristics, and Nyquist criterion. *IEEE Trans. Automatic Control*, pages 145–154, 1986.

[15] J. H. J. H. Lee, C. H. Cho, M. Kim, and J. B. Song. Haptic Interf. through Wave Transformation using Delayed Reflection: Application to a Passive Haptic Device. *Adv. Robotics*, 20(3):305–322, 2006.

[16] N. Diolaiti, G. Niemeyer, and N. A. Tanner. Wave Haptics: Building Stiff Controllers from the Natural Motor Dynamics. *Int. J. Robot. Res.*, 26(1):5–21, 2007.

[17] B. Daunay, A. Abbaci, A. Micaelli, and S. Regnier. The Wave Variables, a Solution for Stable Haptic Feedback in Molecular Docking Simulations. *Innov. Algorithms Techniques Autom. Ind. Electron. Telecom.*, pages 67–73, Springer, 2007.

[18] C. Cho, M. Kim, C. S. Hwang, J. Lee, and J. B. Song. Stable Haptic Display of Slowly Updated Virtual Environment with Multirate Wave Transform. *IEEE/ASME Trans. Mechatronics, 13(5):566–575*, 2008.

[19] J. Ryu, C. Preutsche, B. Hannaford, and G. Hirzinger. Time domain passivity control with reference energy following. *IEEE Trans. Robot. Autom.*, 18(1):1–10, 2002.

[20] G. Niemeyer. *Using Wave Variables in Time Delayed Force Reflecting Teleoperation*. PhD thesis, MIT, 1996.

[21] P. Berestesky, N. Chopra, and M. W. Spong. Discrete Time Passivity in Bilateral Teleoperation over the Internet. In *Proc. IEEE Int. Conf. Robot. Autom.*, pages 4557– 4564, New Orleans, LA, USA, 2004.

[22] Nikhil Chopra, Mark W. Spong, Ra Hirche, and Martin Buss. Bilateral teleoperation over internet: the time varying delay problem. In *American Control Conf.*, pages 168–173, Denver, CO, U.S.A, 2003.

[23] Rogelio Lozano, Nikhil Chopra, and Mark W. Spong. Passivation of force reflecting bilateral teleoperators with time varying delay. In *8th Mechatronics Forum*, pages 24–26, Entschede, Netherlands, 2002.

[24] N. Chopra and M.W. Spong. Delay-independent stability for interconnected nonlinear systems with finite l_2 gain. In *IEEE Conf. Dec. Control*, pages 3847–3852, New Orleans, LA, USA, 2007.

[25] M. Sha Sadeghi, H.R. Momeni, and R. Amirifar. H_∞ and l_1 control of a teleoperation system via LMIs. *Applied Math. Computation*, 206(2):669–677, 2008.